

A Correspondence-Free Color Chart Design for Color Calibration

Hakki Can Karaimer¹ Rang Nguyen²

¹School of Computer and Communication Sciences (IC), Ecole Polytechnique Fédérale de Lausanne (EPFL)

²Ho Chi Minh City University of Technology

hakki.karaimer@epfl.ch nguyenhomanrang@hcmut.edu.vn

Abstract

Colorimetric calibration computes the necessary color space transformation to map a camera's device-specific color space to a device-independent perceptual color space. Color calibration is most commonly performed by imaging a color rendition chart with a fixed number of color patches with known colorimetric values (e.g., CIE XYZ values). The color space transformation is estimated based on the correspondences between the camera's image and the chart's colors. We present a new approach to colorimetric calibration that does not require explicit color correspondences. Our approach computes a color space transformation by aligning the color distributions of the captured image to the known distribution of a calibration chart containing thousands of colors. We show that a histogram-based colorimetric calibration approach provides results that are on-par with the traditional patch-based method without the need to establish correspondences.

Introduction and Motivation

A camera's raw sensor response is in a device-specific color space related to the spectral sensitivities of the Bayer color filters found on a camera's CMOS. One of the key procedures applied onboard a camera is to convert the camera's color space to a device-independent color space based on human perception – namely the CIE XYZ color space or one of its derivatives. The color space transformation is a combination of a white balance to first account for the scene illumination, followed by a transformation based on the spectral characteristics of the camera's sensor [10]. While cameras perform this colorimetric transformation as part of the in-camera image processing procedure, it is often the case that the onboard colorimetric reproduction is not sufficiently accurate, as shown in Figure 1-(A).

To improve the colorimetric mapping of a camera, especially for a particular scene illumination, a calibration procedure is required in order to compute a more accurate color space mapping. The most common procedure is based on the color rendition chart method introduced in 1976 for use with film cameras [13]. This approach relies on color patches with known CIE XYZ properties distributed in fixed locations on the color chart. Using the correspondences between the imaged color chart and color patches on the chart, a mapping between the camera and CIE XYZ can be computed using linear least squares or other optimization strategies. Figure 1-(B) shows the improvements achieved by this conventional patch-based calibration procedure.

This patch-based calibration has been the de facto calibration procedure for over 40 years. While intuitive and simplistic, the approach does have notable drawbacks. The first is that the color space mapping is computed using only a small number of colors. For example, the most commonly used color chart is the Macbeth ColorChecker chart (based on [13]'s original colors) that has only 18 color patches with 6 neutral patches. While these colors are selected to represent a wide spread of the real-

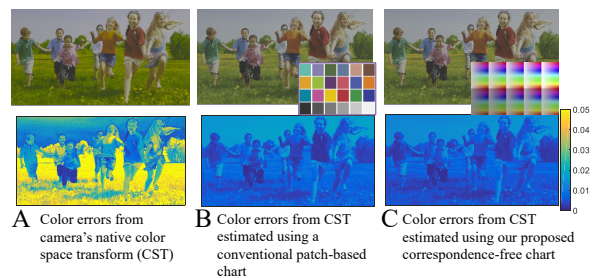


Figure 1. (A) Color matching results based on the camera's onboard color conversion for an LG-G4 camera phone. (B) Result from calibration of the same camera using a patch-based pattern. (C) Result from calibration of the same camera using our proposed correspondence-free pattern.

world colors, they represents a very small sampling of the color gamut. The second and most notable drawback is the need to establish correspondences by localizing the color patches in the camera image. This is generally done by having the user select four corners in the image. This procedure however can be prone to error such as the chart being upside down or partial occlusion. Moreover, this may not be practical for fast and accurate mobile phone imaging requirements.

Contribution This paper reconsiders how color calibration charts are designed. In particular, our goal is to design a color chart that does not require patch localization. To this end, we propose a simple idea of relying on a color histogram of the imaged calibration chart and the known color histogram of the physical pattern in a perceptual color space. This histogram-based strategy allows greater flexibility in calibration pattern design that can incorporate thousands of colors. Key to this approach is a multi-grid optimization strategy that is able to estimate the color space transformation from the input image histogram and the known calibration histogram. We show that this histogram-based approach can produce a color space mapping with accuracy that is on-par with traditional patch-based approach but without the need to localize patches.

Preliminaries and Related Work

Preliminaries Before discussing related work, it is helpful to provide a background on how digital cameras perform their onboard colorimetric mapping. The goal of the color space mapping, also referred to as color space transform (CST), is to map the camera sensor's RGB values to a perceptual color space as if the scene was observed under a reference illumination (e.g., daylight at a 6500K color temperature). As a result, the color space conversion is a combination of the white-balance correction and the color adaptation matrix (CAM) that is related to the spectral characteristics of the camera. Cameras first apply a 3×3 diagonal white-balance matrix (T_{WB}) to correct for the illumination, followed by a 3×3 full CAM matrix (T_{CAM}) that transforms the illumination-corrected raw values into the perceptual color space. We can consider this combined T_{WB} and T_{CAM} to correspond to

the full color space transformation (CST), denoted as \mathbf{T} . As recently discussed by Cheng et al. [2], for most illuminations, the diagonal T_{WB} matrix is capable of correcting only the achromatic colors (thus the name white-balance and not color-balance), and therefore does not properly correct all colors.

Because the initial white-balance correction is only an approximation, cameras generally encode two CAM matrices, T_{CAM}^1 and T_{CAM}^2 , that are computed for sufficiently different illuminations. These different CAMs compensate for the color mapping errors in the white-balance. For an arbitrary illumination, the actual CST is estimated as a combination of the two CAMs that are weighted by the computed white-balance of the scene [10].

This reliance on only two CAMs for two illuminations is one reason the overall color management on a camera is not sufficiently accurate. Because of this, when high-quality colorimetric calibration is required – for example, for professional photographers or medical imaging applications where accurate color reproduction is essential – a calibration procedure is performed under the specific illumination to generate an accurate CST. In such cases, the CST can be computed as a single transformation, although it is still possible to do this as a combination of two separate T_{WB} and T_{CAM} transformations to remain compatible with the standard in-camera processing workflow.

Note that the color space transformation is not the stopping point for the final output. There are several additional steps used to produce the final standard RGB (sRGB) output for JPEG encoding. This involves a number of color manipulation steps, such as tone-mapping and selective color rendering that substantially change the image. More details of the full rendering pipeline can be found in the recent work by [9]. The focus of this paper, however, is on computing an accurate CST.

Related Work The vast majority of previous work for computing a color space transform is based on correspondence obtained from a color chart with standardized samples (e.g., [3–5, 12, 19]). The main difference among these approaches is the technique used to obtain the mapping. For example, Finlayson and Drew [3] proposed a white-point preserving least-squares solution that constrained the CST such that it did not modify corrected achromatic colors. This was improved later by Funt et al. [5] by incorporating perceptual error metrics in the optimization. In a similar vein, Vazquez-Corral et al. [19] proposed using spherical sampling over the LAB color space to estimate the CST. Funt and Bastani [4] proposed a color calibration technique that eliminated the dependence on the scene intensities to handle cases where the color pattern was not well uniformly illuminated.

Another area related to our work is the calibration of a system of cameras. Work by Ilie and Welch [7] proposed a method to calibrate multiple cameras observing the same scene using a closed-loop framework that tunes the camera hardware settings such that the color values of a 24-sample color chart are consistent in all camera images. Work by Nguyen et al. [16] examined the mapping between two cameras’ raw color spaces. In their work, they showed that the mapping is illumination-specific and proposed an illumination-independent mapping approach that uses white-balancing to assist in reducing the number of required transformations.

There are two methods that have utilized color histograms in this multi-camera problem. These methods are intended for multi-camera setups where the cameras are assumed to be observing the same scene content and therefore assume the images should have similar color histograms. In particular, Chen et al. [1] proposed a method to calibrate the multiple cameras

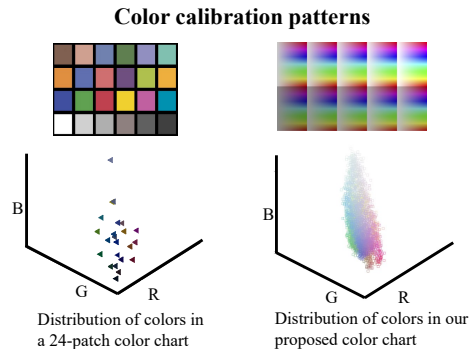


Figure 2. Example of two color charts and their corresponding histograms plotted in the ProPhoto [18] perceptual RGB color space. Two calibration patterns are shown. The first is the standard 24-patch ColorChecker used for conventional color calibration. The other chart is histogram-based pattern used by our method.

by using a simple scale and translation calculated for each color channel based on histogram variation among the camera images. Porikli [17] proposed a much more robust method that computed a per-channel brightness transfer function for a pair of cameras based on the images’ histograms.

Our work is distinguished from prior work in its goal to achieve accurate 3×3 color space transform in a correspondence-free manner. While histogram matching has been used for related problems, to the best of our knowledge it has not been examined as a viable alternative for accurate colorimetric calibration. Moreover, the color calibration pattern design has not changed for over 40 years.

Correspondence-Free Color Calibration

We begin by first describing our overall approach. This is followed by details on our optimization approach to compute the 3×3 color space transformation, \mathbf{T} using 3D color histograms.

Overall Framework

Fig. 2 shows an example of two calibration chart, one based on traditional 24 colors and the other representing color distribution-based charts used by our proposed method. The colors of the charts are plotted in the wide-gamut ProPhoto [18] color space that is commonly adopted in lieu of CIE XYZ. As with all calibration methods, our starting assumption is that we are given a color chart with known colorimetric values. These values can be established using a spectroradiometer or colorimetric calibrated device.

Fig. 3 shows a high-level diagram of the overall procedure for our approach. Fig. 3-(A) shows the traditional correspondence-based method that can directly solve a linear system for the \mathbf{T} . Fig. 3-(B) shows our strategy that aligns the histograms of the known color chart distribution and an image from a camera. The histogram alignment procedure is described in the following section.

Histogram Alignment

The main idea of our approach is to compute the transformation matrix \mathbf{T} between the source and destination histograms. Our input contains a raw RGB image of the color pattern I_s that is extracted from the input image, and the distribution of the colorimetric values on the of the calibration pattern I_d . The transformation matrix is computed by minimizing the following cost function:

$$\mathbf{T} = \arg \min_{\mathbf{T}} \mathcal{D}(\mathcal{H}(I_d, n) || \mathcal{H}(\mathbf{T} \times I_s, n)), \quad (1)$$

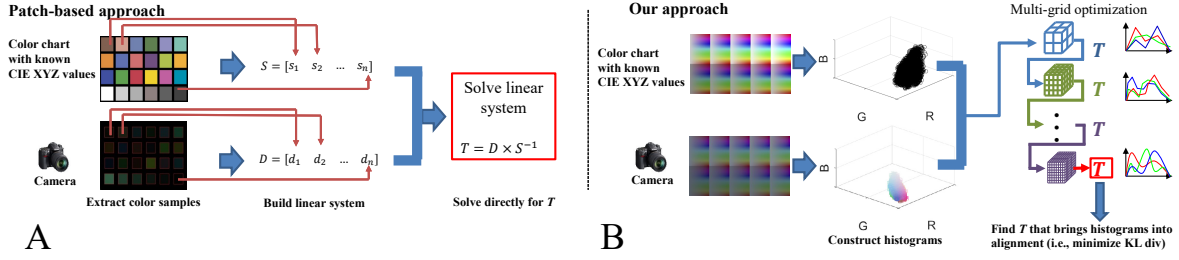


Figure 3. This figure shows a comparison between color chart approach and our histogram-based approach. (A) *Color chart*: Color samples image of a chart provides RAW RGB correspondences such that \mathbf{T} can be solved by a direct linear system. (B) *Our approach*: Images of the same pattern provide color samples. The camera’s color distribution should be similar to the distribution of the color chart. Multi-scale optimization is used to compute a \mathbf{T} that brings the two histograms in alignment by minimizing the KL divergence.

where the function $\mathcal{H}(I, n)$ is the normalized 3D histogram of an image (or distribution) I with the number of bins n , and the distance $\mathcal{D}(P||Q)$ is the Kullback-Leibler (KL) divergence distance between the two 3D histograms which is defined as follows:

$$\mathcal{D}(P||Q) = \sum_{r,g,b} \log \left(\frac{P(r,g,b)}{Q(r,g,b)} \right) P(r,g,b), \quad (2)$$

where r, g, b are indices for red, green, and blue channel respectively. It is also worth noting that these histograms are normalized such that the summation is equal to 1.

To solve the transformation matrix \mathbf{T} in Eq. 1, we use the Nelder-Mead simplex method [11, 14] implemented in the `fminsearch` function of Matlab. The minimization is initialized using one of three different initializations as described in the accompanying supplemental material. Directly optimizing Eq. 1, however, can get stuck in a local minimum depending on the starting point since this cost function is non-convex. To overcome this, we use a multi-grid optimization approach where the optimization is run repeatedly with increasing the number of histogram bins 2^k (where $k = 4, 5, \dots, 8$). In addition, at each iteration, each row of the matrix \mathbf{T} is optimized independently as follows:

$$\mathbf{T}(c, :)^{(k)} = \arg \min_{T(c, :)} \mathcal{D}(\mathcal{H}(I_d, 2^k) || \mathcal{H}(\mathbf{T} \times I_s, 2^k)), \quad (3)$$

where c is the index for the row number. This is equivalent to minimizing the cost function over the marginal probabilities of the 3D histograms color channels. It is also worth noting that the initial matrix for the current iteration is set to the output matrix of the previous iteration. The pseudo-code for this optimization approach is provided in Alg. 1.

Algorithm 1 Multi-scale Histogram Alignment

Input: raw RGB image of the color pattern I_s , the distribution of the colorimetric values on the color pattern I_t .

- 1: Initialize $\mathbf{T}_{\text{init}}^{(1)}$ as described in the supplemental material
- 2: **for** $k = 4$ to 8 **do**
- 3: **for** $c = 1$ to 3 **do**
- 4: Optimize the row c^{th} of $\mathbf{T}^{(k)}$ based on Eq. 3 starting with matrix $\mathbf{T}_{\text{init}}^{(k)}$
- 5: **end for**
- 6: $\mathbf{T}_{\text{init}}^{(k+1)} \leftarrow \mathbf{T}^{(k)}$
- 7: **end for**

Output: the transformation matrix \mathbf{T} .

Experimental Results

This section performs two different experiments to demonstrate the effectiveness of our new color pattern design. The first

is based directly on the spectral reflectance of a real MacBeth chart. The second is a proof of concept experiment based on patterns constructed and printed at a commercial printing service.

Synthetic chart

Because it is challenging to construct a physical chart using the same type of materials as used in the MacBeth color rendition chart, we first perform an experiment using synthetic images based on the spectral power distributions measured on the Macbeth Color rendition chart. To do this, we have measured the spectral power distributions (SPD) of the color rendition patches using a Specim’s PFD-CL-65-V10E hyperspectral camera. We have access to the CIE XYZ matching functions [6] and the spectral sensitivities of a number of cameras [8].

We can generate the tristimulus response of image I and channel c for each patch’s SPD as follows:

$$I(c) = \int_{\omega} R_c(\lambda) S_i(\lambda) L(\lambda) d\lambda, \quad (4)$$

where λ represents the wavelength, ω is the visible spectrum 380 to 720nm, R_c is the tristimulus response (e.g., a camera’s spectral sensitivities or the CIE XYZ matching functions), and c is the three stimulus channel (e.g., $c = r, g, b$ or $c = X, Y, Z$). The term $S(\lambda)_i$ represents the spectral power distribution of patch i and $L(\lambda)$ is the lighting in the scene which is assumed to be spatially uniform.

As shown in Figure 4, we synthesize camera images and CIE XYZ targets using the measured spectral power distributions of MacBeth colour patches. By blending synthetic pairs of the original color patches we generate our pattern. We compute the required transformations using those synthetic colour charts using three methods: (1) linear least squares based on the 24 color patches, (2) Funt and Bastani [4] based on the 24 color patches, and (3) our histogram-based method without correspondence. Our results are tested on scenes captured by [15]. We see that our results obtained with our histogram-based method are comparable to the two based on color correspondences.

Prototype with printed charts

Next we perform experiments with printed color charts. To provide a fair comparison of the patch-based method against the proposed histogram-based method we use the following procedure for all of our experiments in this section. The two calibration patterns (i.e., the 24-patch pattern based on the Macbeth Color Chart and the histogram-based chart as shown in Fig. 2) are created in the CMYK color space and printed on matte paper. All patterns are printed using the same commercial printing service to ensure they are of the same materials. These printed calibration patterns are used as the calibration targets for our experiments. To test the quality of our results, we use three test

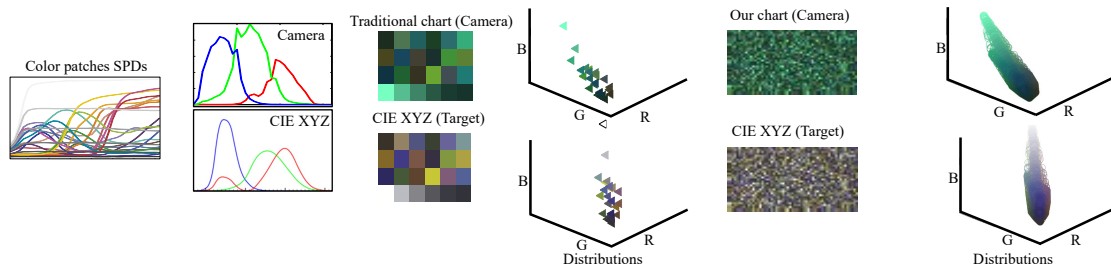


Figure 4. This figure illustrates our procedure to produce synthetic color charts based on the spectral power distributions (SPD) of the MacBeth color patches. Using the spectral sensitivities of a camera and the CIE XYZ color matching functions, we can generate camera images and their CIE XYZ target. To generate our pattern, we blend pairs of the original color patches to produce thousands of colors.

Method	Average Euclidean error
Linear least squares	0.0132
Funt and Bastani [4]	0.0134
Ours	0.0139

The table shows the comparisons of average Euclidean error between linear least squares, Funt and Bastani [4], and our histogram based approach using 18 hyperspectral scenes from [15].

images (see supplemental material) printed on matte paper. The color calibration pattern and test images are imaged by four different camera phones: Google Nexus 6, Samsung S6-Edge, LG-G4, Apple iPhone 7.

To establish the ground-truth for each camera and illumination, each camera is calibrated using the X-rite Color calibration software [20] which is an industry standard in camera color management. To do this, each camera captures an image of the X-rite ColorChecker Chart under each illumination. We then generate an Adobe DNG (common on mobile devices) profile that is able to convert the camera’s raw image to the Prophoto color space. The X-rite colorimetric mapping involves both a 3×3 CST and a non-linear 3D look up table (LUT) to correct the camera’s colors. This additional LUT provides a high-quality colorimetric mapping of the images scene. We acknowledge that this means our correspondence-free approach is reliant on a correspondence-based method to establish the ground-truth for comparison; however, we believe this setup provides a fair imaging setup to validate the proposed idea.

Calibration Comparisons

Table 1 shows the average of Euclidean errors for 18 hyperspectral scenes from [15]. As showed in Fig. 5, the compared methods by linear least squares, Funt and Bastani [4], and our histogram based approach provides similar results.

Fig. 6 shows the results for all the four camera phones. The figure shows the error map of the camera’s native CST, the CST estimated using least squares fit together with Funt and Bastani [4] of the color patches, and our histogram-based method with the our color chart design. The corresponding number is the average error over test image 1. Similar results for test image 2 and 3 are provided in the accompanying supplemental material. The error maps reveal that the proposed correspondence-free calibration approach provides results that are on-par with the conventional patch-based method. It should be noted that since Funt and Bastani [4] have to scale CST based on the brightness of the scene, this may affect their final outcome.

Robustness

We examine the situation where part of the calibration pattern is occluded. Our histogram-based method with the redundant color design is naturally more robust to this situation and is

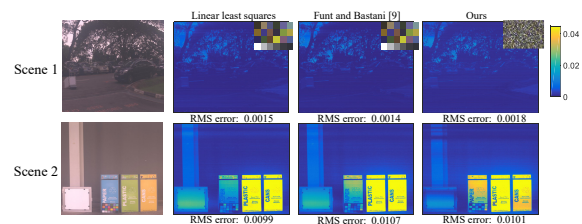


Figure 5. This compares the colorimetric calibration results for the synthesized 24-patch colour chart and our pattern obtained by blending for three methods (linear least squares, Funt and Bastani [4], and our histogram-based method). Compared is the CST estimated from a 24-patch color chart, and our results based on our chart design (see supplemental materials for the remaining test scenes error maps).

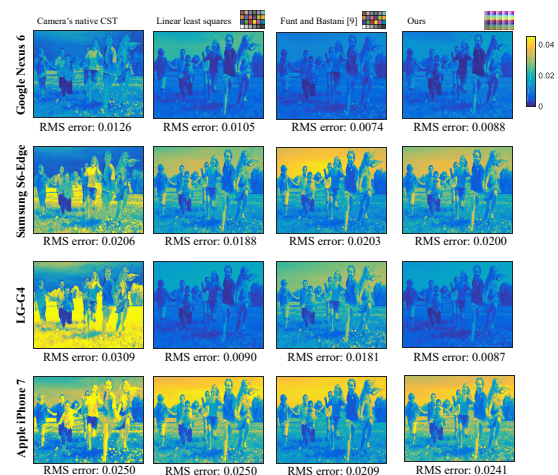


Figure 6. This figure compares the colorimetric calibration results for the four camera phones. Compared is the camera’s native CST, the CST estimated using least squares fit together with Funt and Bastani [4] of the color patches, and our histogram-based method with the our color chart design. The error map is for test image 1 (see supplemental materials for the test images 2 and 3).

still able to estimate a high-quality CST to improve the camera. Please see our supplemental material for this experiment.

Discussion and Conclusion

We have presented a correspondence-free approach to colorimetric calibration. The main contribution of this paper is to demonstrate that color charts designed for use with a histogram-based optimization are a viable alternative to the 40+ year-old conventional method requiring explicit correspondence with color patches. We have shown that in many cases the histogram-based approach can produce a more accurate mapping than patch-based methods. In addition, the histogram-based approach offers advantage of requiring no explicit correspondence and robustness to occlusion.

References

- [1] Y. Chen, C. Cai, and J. Liu. Yuv correction for multi-view video compression. In *ICPR*, 2006. 2
- [2] D. Cheng, B. Price, S. Cohen, and M. S. Brown. Beyond white: Ground truth colors for color constancy correction. In *ICCV*, 2015. 2
- [3] G. D. Finlayson and M. S. Drew. White-point preserving color correction. In *CIC*, 1997. 2
- [4] B. Funt and P. Bastani. Irradiance-independent camera color calibration. *Color Research & Application*, 2014. 2, 3, 4
- [5] B. Funt, R. Ghaffari, and B. Bastani. Optimal linear rgb-to-xyz mapping for color display calibration. In *CIC*, 2004. 2
- [6] J. Guild. The colorimetric properties of the spectrum. *Philosophical Transactions of the Royal Society of London*, 230:149–187, 1932. 3
- [7] A. Ilie and G. Welch. Ensuring color consistency across multiple cameras. In *ICCV*, 2005. 2
- [8] J. Jiang, D. Liu, J. Gu, and S. Süsstrunk. What is the space of spectral sensitivity functions for digital color cameras? In *WACV*, 2013. 3
- [9] H. Karaimer and M. S. Brown. A software platform for manipulating the camera imaging pipeline. In *ECCV*, 2016. 2
- [10] H. C. Karaimer and M. S. Brown. Improving Color Reproduction Accuracy on Cameras. In *CVPR*, 2018. 1, 2
- [11] J. C. Lagarias, J. A. Reeds, M. H. Wright, and P. E. Wright. Convergence properties of the nelder–mead simplex method in low dimensions. *SIAM Journal on Optimization*, 9(1):112–147, 1998. 3
- [12] F. Martinez-Verdu, J. Pujol, and P. Capilla. Characterization of a digital camera as an absolute tristimulus colorimeter. *Journal of Imaging Science and Technology*, 2003. 2
- [13] C. S. McCamy, H. Marcus, , and J. G. Davidson. A color-rendition chart. *Sensors*, 2(3):95–99, 1976. 1
- [14] J. A. Nelder and R. Mead. A simplex method for function minimization. *The Computer Journal*, 7(4):308–313, 1965. 3
- [15] R. M. Nguyen, D. K. Prasad, and M. S. Brown. Training-based spectral reconstruction from a single rgb image. In *ECCV*, 2014. 3, 4
- [16] R. M. H. Nguyen, D. K. Prasad, and M. S. Brown. Raw-to-raw: Mapping between image sensor color responses. In *CVPR*, 2014. 2
- [17] F. Porikli. Inter-camera color calibration by correlation model function. In *ICIP*, 2003. 2
- [18] K. E. Spaulding, E. Giorgianni, and G. Woolfe. Reference Input/Output Medium Metric RGB Color Encodings (RIMM/ROMM RGB). In *Image Processing, Image Quality, Image Capture, Systems Conference*, 2000. 2
- [19] J. Vazquez-Corral, D. Connah, and M. Bertalmío. Perceptual color characterization of cameras. *Sensors*, 14(12):23205–23229, 2014. 2
- [20] X-Rite. *X-Rite ColorChecker Camera Calibration software*, accessed December 11, 2019. https://xritephoto.com/ph_product_overview.aspx?action=support&id=2632. 4